Front. Phys. China, 2010, 5(3): 245–259
DOI 10.1007/s11467-010-0105-8

REVIEW ARTICLE

Spontaneous emission in micro- and nano-structures

Jing-feng LIU (刘景锋)[1,2], **Xue-hua WANG** (王雪华)[1,†]

[1] *State Key Laboratory of Optoelectronic Materials and Technologies, School of Physics and Engineering, Sun Yat-Sen University, Guangzhou 510275, China*
[2] *College of Science, South China Agriculture University, Guangzhou 510642, China*
E-mail: wangxueh@mail.sysu.edu.cn

Received May 24, 2010; accepted June 6, 2010

Spontaneous emission of emitters governing the performance of optoelectronic devices is a fundamental phenomenon, and it has strong environment-dependent characteristics. In this article, we mainly review the experimental and theoretical progresses in the control of spontaneous emission by manipulating optical modes with photonic crystals, optical microcavities and metallic nanostructures. The spontaneous emission from emitters in photonic crystals can be modified by the local density of states, and by employing photonic crystals, the devices' efficiency is enhanced, the angular radiation pattern can be engineered, and highly efficient optoelectronic devices are achieved through decreasing the radiative lifetime. In quantum optical devices, microcavities would alter the lifetime of an excited state through tuning the resonance in the frequency and positioning between the emitters and cavity field, and inducing the emitters to emit spontaneous photons in a desired direction. The emerging enhanced electromagnetic field near metallic nanostructures can help to control and manipulate the spontaneous emission of an emitter. The use of micro- and nano-structures to manipulate spontaneous emission will open unprecedented opportunities for realizing functional photonic devices.

Keywords spontaneous emission, photonic crystals, optical microcavity, metallic nanostructures, local density of states, quantum dots

PACS numbers 42.50.ct, 32.80.-t, 42.70.Qs

Contents

1 Introduction

Spontaneous emission (SE) is a fundamental process that plays an essential role in many phenomena in nature, by which a light emitter in an excited state undergoes a transition to the ground state and emits a photon. The SE manipulation investigation is an all-important research direction in quantum optics. This is because it may limit the performance of optoelectronic devices in a diverse range of applications such as solar energy harvesting [1–5], optical communications and single photon sources for quantum information [6–13]. The performance of LEDs [14], for example, is severely limited by a large amount of the SE photons in the material that are not extracted from the devices. Similarly, the threshold of a laser [15] will be raised because of spontaneously emitted photons not coupling to the lasing mode, and the speed of laser modulation is also limited by the SE. Therefore, it is important to manipulate SE and inhibit it when it is not desired. Therefore, engineering SE can be considered as an important project in the photonics research field, which will lead to dramatic advances

regarding both efficiency as well as speed in photonic devices.

In 1946, Purcell predicted the enhancement of the SE rate of emitters when they are placed in a resonant cavity (the Purcell Effect) [16]. Following this concept, it has become well known that the rate of SE has a strong environment-dependent characteristic and is proportional to the photonic local density of states (LDOS). Therefore, the key of manipulating the SE is to tailor LDOS of electromagnetic waves and the spatial distribution relative to the emitters.

Photonic crystals (PCs) are periodic dielectric structures with variations in the refractive index on the scale of the order of the light wavelength, which may lead to photonic band gaps. The characteristics can be analogous to electronic band gaps properties for electrons moving in the periodic electrostatic potential of semiconductor crystal structures. The optical modes can be fine controlled through engineering the periodicity of the lattice, the filling ratio of PCs, or the refractive-index of the material. Consequently, the PCs can manipulate the emission of emitters. As a result, since the pioneering work of Yablomovitch [17] and John [18], controlling of light emission using PCs has received increasing interest in experiments [19–27] and theories [28–38]. Noda's group has been achieving rapid progress in SE control by three- [19] or two-dimensional [39–42] (3-D or 2-D) PCs.

An optical microcavity is an optical resonator close to, or below the dimension of the wavelength of light, which can confine light to a small volume and is very suitable to control the radiation properties of emitters. According to different applications, microcavities have different geometrical types. A review about microcavity geometrical structures and characteristics had been given in detail by Vahala [43]. Kavokin [44] presented diverse microcavities made by semiconductor, metallic and dielectric structures and briefly described their characteristics corresponding to microcavities. According to Cavity Quantum Electrodynamics (CQED) theory [45], two different strength coupling regimes can be reached, depending on the coupling strength between the emitter and the optical microcavity mode. In weak-coupling regime, the emitter SE rate can be altered by the Purcell effect [16] and the SE photons can be tailored to emit in a desired direction. Weak-coupling between an emitter and a microcavity has been demonstrated using micropillars [46–50], microdisks [51–53], and PCs microcavities [10, 54–56]. In strong coupling regime, the SE process is changed into a reversible energy-exchange process between the emitter and the microcavity, in which Purcell effect is no longer active. In this case, the quantum coherent superposition [57] between the emitter's quantum states and microcavity modes is possible, which is a base for future quantum information processing. Many exciting experiment results have been recently observed in microwave cavity [58], micropillar [59–62], microdisk [63–65], and PC microcavities [66–69]. In microcavities, Vacumm Rabi Splitting [70] was observed through strong interaction. Recently, Reithmainer gave a detailed presentation [71] on strong exciton–photon coupling in semiconductor and microcavities systems.

It is interesting in manipulating light quanta, and in engineering devices for potential applications including efficient photon collection and long-range entanglement realization. Metallic micro- or nano-structures can provide another cavity-free approach to control the interaction between the emitter and sub-wavelength confinement of the optical field. In recent years, both in experiments and theories, there have been a growing interest in controlling the efficiency of SE using metallic micro- or nano-structures, such as thin noble metal nanofilms [72–77], nanowires [78–84], and nanoparticles [85, 86].

This review focuses on SE phenomena in micro- or nano-structures, such as 2-D and 3-D PCs, microcavities and metallic nanostructures. Such structures offer the ability to control both radiation pattern and the relaxation time of the emitters. The paper is structured as follows: in Section 2, we present theoretical researches on SE in PCs, microcavities, and metallic nanostructures. In Section 3, experimental findings about SE control are demonstrated. Finally, conclusions and the outlook are given.

2 Theoretical treatment on SE in micro- and nano-structures

In this section, we present the theoretical description on the dynamic decay processes of the emitters in micro- or nano-structures.

2.1 Generalized up-level evolution formula in PCs

Since 1990, the isotropic and anisotropic dispersion models have been extensively employed to solve the QED problems in PCs. Many novel quantum optics characteristics have been predicted [87] using them. However, these two models only simulate the dispersion relation extremely close to the band edges, and furthermore ignore the strong space inhomogeneity of the electromagnetic field in PCs. On the other hand, it has been recognized that the LDOS is more decisive for emission behavior of emitters in inhomogeneous media [32, 35], when the position-dependent interaction between photons and emitters is taken into account. Because different experiments observed different lifetime distributions [88–91], to clearly understand these discrepancies, Wang *et al.* for the first time introduced a lifetime distribution function for an assembly of emitters in 3-D PCs with pseudo gap [34]. Their numerical simulations show that quite wide

or narrow lifetime distributions can occur for different spread configurations of the emitters. The pure PCs effect may lead to the coexistence of both accelerated and inhibited decay processes. These results provide theoretical clarification for substantial discrepancies in the different experimental observations.

First, we consider the decay behavior of a single emitter. Then, we introduce a lifetime distribution function for an assembly of emitters. We consider the SE of a two-level emitter located at the position $\boldsymbol{r}$ in PCs. Hamiltonian of the system can be presented in the form:

$$H = \hbar\omega_0 b_2^+ b_2 + \hbar\sum_{n\boldsymbol{k}} \omega_{n\boldsymbol{k}} a_{n\boldsymbol{k}}^+ a_{n\boldsymbol{k}} + \hbar\sum_{n\boldsymbol{k}} [g_{n\boldsymbol{k}}(\boldsymbol{r}) b_1^+ b_2 a_{n\boldsymbol{k}}^+ + g_{n\boldsymbol{k}}^*(\boldsymbol{r}) b_2^+ b_1 a_{n\boldsymbol{k}}] \quad (1)$$

In Eq. (1), b_i and $b_i^+ (i = 1, 2)$ are annihilation and creation operators of electron in the ground and excited states, respectively, $a_{n\boldsymbol{k}}$ and $a_{n\boldsymbol{k}}^+$ are annihilation and creation operators of the photon; ω_0 is the emitter transition frequency; $\omega_{n\boldsymbol{k}}$ is the frequency of the electromagnetic (EM) field eigenmode $\boldsymbol{E}_{n\boldsymbol{k}}(\boldsymbol{r}) = \mathrm{i}c \times \boldsymbol{H}_{n\boldsymbol{k}}(\boldsymbol{r})/[\varepsilon(\boldsymbol{r})\omega_{n\boldsymbol{k}}]$ in PCs, which can be found by the plane-wave expansion method [92]. $g_{n\boldsymbol{k}}(\boldsymbol{r})$, the coupling coefficient, given by

$$g_{n\boldsymbol{k}}(\boldsymbol{r}) = \mathrm{i}\omega_0 (2\varepsilon_0 \hbar\omega_{n\boldsymbol{k}} V)^{-1/2} \boldsymbol{E}_{n\boldsymbol{k}}(\boldsymbol{r}) \cdot \boldsymbol{\mu}_d \quad (2)$$

where $\boldsymbol{\mu}_d = \mu_d \hat{\mu}$ is the dipole transition moment of the emitter between two levels.

We assume that the emitter is initially excited at its upper level and there is no photon in the EM field, and denote $|I\rangle = |2, 0\rangle$ and $|F_{nk}\rangle = |1, n\boldsymbol{k}\rangle$ as the initial and final states of the system, respectively. The state vector of the system evolves in terms of

$$|\psi(t)\rangle = C_2(t)|I\rangle + \sum_{n\boldsymbol{k}} C_{1,n\boldsymbol{k}}(t)|F_{nk}\rangle = U(t)|I\rangle \quad (3)$$

with the initial conditions $C_2(0) = 1$ and $C_{n\boldsymbol{k}}(0) = 0$, where $U(t)$ is the evolution operator. Applying the Green's function technique to the evolution operator, we obtain [93]

$$C_2(\omega) = \frac{1}{2\pi\mathrm{i}}[G_{ii}^- - G_{ii}^+] \quad (4)$$

where $G_{ii}^{\pm} = \lim_{\eta\to 0}\langle I|G(z = \omega \pm \mathrm{i}\eta)|I\rangle$ with the resolvent $G(z) = (z - H/\hbar)^{-1}$. Note that with the nonvanishing matrix elements, we can analytically obtain

$$G_{ii}^{\pm} = \frac{1}{\omega - \omega_0 - \Delta(\boldsymbol{r}, \omega) \pm \mathrm{i}[\Gamma(\boldsymbol{r}, \omega)/2 + \eta]} \quad (5)$$

with $\Gamma(\boldsymbol{r}, \omega) = \dfrac{\pi\omega_0^2\mu_d^2}{3\varepsilon_0\hbar\omega}\rho(\boldsymbol{r}, \omega)$ (6)

$$\Delta(\boldsymbol{r}, \omega) = \frac{1}{2\pi} P\int_0^{\infty} \frac{\Gamma(\boldsymbol{r}, \omega')}{\omega - \omega'}\mathrm{d}\omega' \quad (7)$$

where ω_0 is the emitter transition frequency and P represents the integral principle value. In Eq. (6), the local density of photonic states is defined as:

$$\rho(\boldsymbol{r}, \omega) = \frac{1}{(2\pi)^3}\sum_n \int_{\mathrm{FBZ}} \mathrm{d}\boldsymbol{k}|\boldsymbol{E}_n(\boldsymbol{k}, \boldsymbol{r}) \cdot \hat{\mu}|^2 \delta(\omega - \omega_{n\boldsymbol{k}}) \quad (8)$$

Combing Eq. (4) with Eq. (5), we find that the decay of an excited emitter can be described by

$$C_2(t) = \int_{-\infty}^{\infty} \mathrm{d}\omega C_2(\omega)\mathrm{e}^{-\mathrm{i}\omega t} \quad (9)$$

with

$$C_2(\omega) = \frac{1}{\pi}\lim_{\eta\to 0^+} \frac{\Gamma(\boldsymbol{r}, \omega)/2 + \eta}{[\omega - \omega_0 - \Delta(\boldsymbol{r}, \omega)]^2 + [\Gamma(\boldsymbol{r}, \omega)/2 + \eta]^2} \quad (10)$$

That $\Gamma(\boldsymbol{r}, \omega)$ and $\Delta(\boldsymbol{r}, \omega)$ represent the local coupling strength (LCS) and the level shift, respectively.

The calculation of $\rho(\boldsymbol{r}, \omega)$ in Eq. (8) involves an integral of the EM fields in the first Brillouin zone (FBZ). This is a time consuming task. We have established an exact and time saving numerical method [94] for the evaluation of integrals of vectorial fields in PCs.

2.2 Lifetime distribution for an assembly of emitters in 2-D PCs

Next, we apply the theory addressed above to study the SE of emitters in 2-D or 3-D PCs. For describing the lifetime distribution of the SE caused by the effect of PCs and investigating the dynamic processes of the SE, the lifetime distribution function (LDF) has been defined [34]. Along the height direction of the 2-D PCs is translation invariance. Thus, the SE in the 2-D PCs may not be forbidden completely because the SE light may travel along the height direction of the rods and escape out of the 2-D periodic plane. Therefore, the properties of SE in the 2-D PCs are governed by the actual 3-D LDOS of the 2-D PCs, rather than the 2-D LDOS. InPCs, the LDF is defined as [36]:

$$\rho(\tilde{\tau}) = \sum_i W_i \frac{1}{\sqrt{\pi}\sigma}\exp\{\frac{-[\tilde{\tau} - \tilde{\tau}(\boldsymbol{r}_i, \omega)]^2}{\sigma^2}\} \quad (11)$$

where $\tilde{\tau}(\boldsymbol{r}_i, \omega) = \tau(\boldsymbol{r}_i, \omega)/\tau_f(\omega)$, $\tau(\boldsymbol{r}_i, \omega)$ and $\tau_f(\omega)$ are the SE lifetime at a given position $\boldsymbol{r}_i$ in PCs and in homogeneous medium, respectively. The symbol W_i denotes the weight factor. In the cases of homogeneous distribution of emitters in space, we choose $W_i = 1$. The summation runs over all the considered excited emitters, where we let $\sigma = 0.05$, which is enough to guarantee the smoothness of the LDF curves. $\tau(\boldsymbol{r}_i, \omega)$ is given by the following equation:

$$\tau(\boldsymbol{r}, \omega) = \frac{1}{\Gamma(\boldsymbol{r}, \omega)} \quad (12)$$

First, we consider a 2-D square lattice PC composed of square air rods in the dielectric medium of the dielectric constant $\varepsilon = 12.96$. Each square rod is rotated an

angle of $\theta = 30^\circ$ around its symmetric axis in the height direction. In the following calculations, all the above structural parameters are fixed except for different filling factors of $f = 0.4$, 0.6, 0.68 and 0.75. In the case of $f = 0.68$, the 2-D PC possesses the largest pseudo-PBG of $\Delta\omega = 0.063(2\pi c/a)$ (in this review a denotes the lattice constant and c the light speed in vacuum) with a midgap frequency of $\omega_g = 0.425(2\pi c/a)$ [95]. Therefore, we pay attention to two special frequencies: the midgap of $\omega_g = 0.425(2\pi c/a)$ and the pseudoband edge of $\omega_l = 0.385(2\pi c/a)$.

Figure 1(a) and (b) displays the LDFs of the excited emitters located in the background medium and in the air rods of the PCs, respectively. In calculation, we choose $\omega = \omega_g = 0.425(2\pi c/a)$ as the emitters' transition frequency. In order to demonstrate the pure PCs effect, the reference lifetimes τ_f is respectively chosen as that of the emitters in homogeneous background medium for Fig. 1(a) and in vacuum for Fig. 1(b), which is shown by the vertical dashed-line located at $\tilde{\tau} = 1$ in Fig. 1. Two notable results can be observed from Fig. 1(a): (i) the LDFs in each case has quite wide distribution. It implies that the SE behavior in the 2-D PCs is no longer described by a single lifetime. (ii) Compared with the case of emitters in the homogeneous medium of $\varepsilon = 12.96$, all the SE are almost inhibited. The SE lifetimes gradually become long as the filling factor f increases from 0.4 to 0.68. But when $f = 0.75$, the inhibition effect of the SE in the PCs is weakened. These results can be well understood when we note that the structure of $f = 0.68$ possesses the largest pseudo-PBG and the atomic transition frequency is just located at the center of the largest pseudo-PBG. When the filling factor goes away from $f = 0.68$, the width of the pseudo-PBG of the corresponding PCs is narrowed down and the atomic transition frequency deviates from the center of the pseudo-PBG. Therefore, the inhibition effect of the SE in the non-optimal structures is significantly weakened. In Fig. 1(b), all the curves show quite wide lifetime distribution, as illustrated in Fig. 1(a). Two differences from Fig. 1(a) should be addressed. One is that for the structure of $f = 0.4$, the reduced lifetimes almost distribute in the range of $\tau < 1$, which manifests that most SE now are accelerated. The other is that for the structures of $f = 0.6$, 0.68 and 0.75, the lifetimes of some emitters are decreased and the others are increased, which reveals that both the acceleration and the inhibition processes coexist in these PC samples. It is not surprising that a considerable difference occurs in Fig. 1(a) and (b). The electric fields of the eigen modes are discontinuous at interfaces, for instance, the electric fields in the air rods are larger than that in the dielectric medium. This leads to sudden enhancement of the LDOS near interfaces in the air rods, which gives rise to the inhibition or acceleration process of the SE in the high or low refractive index medium. Combined with the position-dependent fluctuations of the LDOS, these results in Fig. 1(b) can be well understood. Now, we turn to examine the case of $\omega = \omega_l = 0.385(2\pi c/a)$, i.e., the emitters' transition frequency is located at the pseudo-band edge of the optimal structural sample of $f = 0.68$. The numerical results of the LDFs are displayed in Fig. 2(a) and (b) corresponding to the emitters randomly spread in the dielectric background medium or in air rods, and the reference lifetime is the same as that in Fig. 1(a) and (b). In Fig. 2(a), the curve of $f = 0.68$ shows that the lifetime distribution becomes narrow and the emitters SE almost are accelerated. As it is well known that the band edges enhance the SE because the LDOS reaches its maximum near the band edges in 3-D PCs. It is reasonable to expect that the pseudo-band edges of 2-D PCs have a similar effect. On the other hand, for the other three structures, the emitters' transition frequency goes away from the pseudo-band edges of these structures, thus, the LDOS is reduced and the pseudo-band edges' effect is substantially weakened. In addition, high

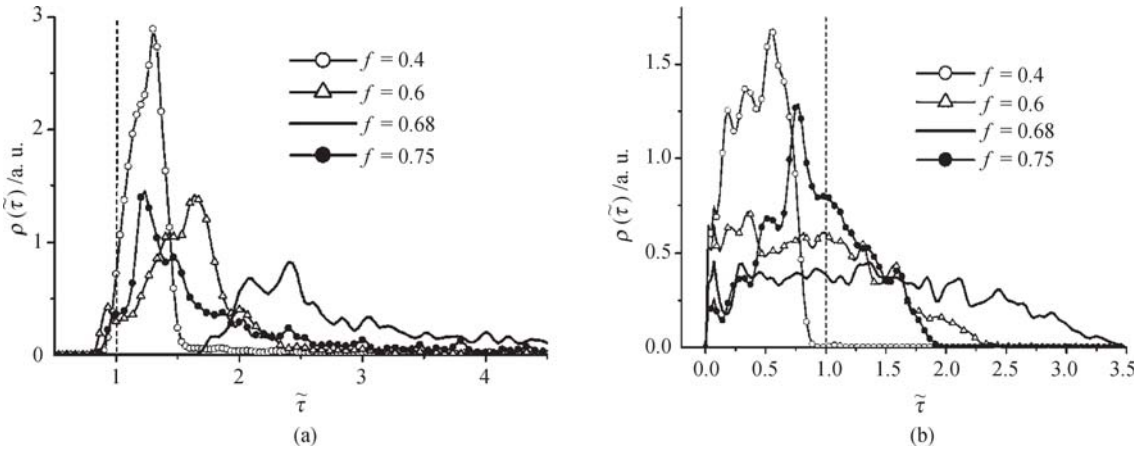

Fig. 1 Lifetime distribution for the emitters with the transition frequency $\omega = 0.425(2\pi c/a)$ in the 2-D PCs composed of square air rods in the background medium $\varepsilon = 12.96$ with different filling factors $f = 0.4$, 0.6, 0.68 and 0.75. **(a)** The emitters homogeneously spread over the background medium and **(b)** the emitters distribute in the air square rods.

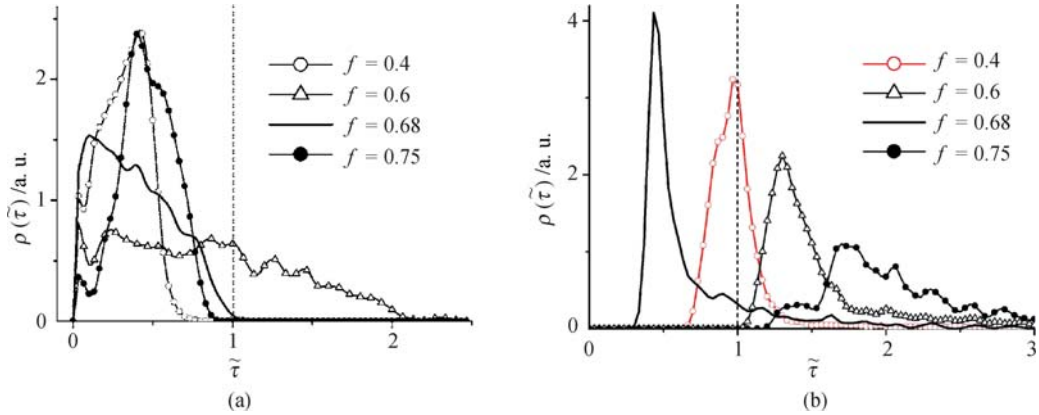

Fig. 2 Lifetime distribution for the emitters with the transition frequency $\omega = 0.385(2\pi c/a)$ in the 2-D PCs with same parameters as Fig. 1. **(a)** For the emitters in the background medium and **(b)** for the emitters in air square rods.

refractive index of the dielectric medium also leads to the reduction of the LDOS, which results in the suppression of the SE process. Consequently, for the other three structures, the SE enhanced effect should be gradually weakened, i.e., the SE suppression effect becomes dominant. These arguments are just confirmed by the results displayed in Fig. 2(a). On the other hand, Fig. 2(b) shows the LDFs of emitters embedded in air rods. Except for the sample of $f = 0.6$, the SE of the emitters in other samples are accelerated. Among them, the SE enhanced effect in the optimal structure of $f = 0.68$ is most remarkable due to the presence of a large LDOS in the air rods caused by the pseudo-band edges and the dielectric discontinuity. The curve of 0.75 in Fig. 2(b) is different from the corresponding curves in Fig. 1(b). It does not contain any inhibition component of the SE because the transition frequency of $\omega = 0.385(2\pi c/a)$ is located outside pseudo-PBG, thus, the inhibition process can not occur. Why does the curve of $f = 0.6$ lie across the dashed line with a wide profile? We calculate the pseudo-PBG for this PC sample and find that its pseudo-PBG spreads over the frequency range of $[0.375, 0.395]2\pi c/a$. The atomic transition frequency $\omega = 0.385(2\pi c/a)$ falls within the pseudo-PBG. Therefore, both the enhanced effect caused by the dielectric discontinuity and the inhibition effect generated from the pseudo-PBG coexist, similar to the case appearing in Fig. 1(b).

By tuning the polarization orientation of the emitters, we find the switching effect of emitters SE in 2-D PCs [37]. We also consider a 2-D square lattice PC consisting of square air rods in background medium with the permittivity being the same as Fig. 1. As drawn in Fig. 3, in which a Wigner–Seitz cell is surrounded by the dashed line, the air rods are represented by the blank areas, a is the lattice constant, and θ is the rotation angle of the air rods with respect to the x axis. We choose the parameters as follows: $f = 0.68$ and $\theta = 30°$. In this situation, the PCs have the largest pseudo-PBG [95]. In our calculations, we assume that 10 000 excited atoms distribute homogeneously in a unit cell, which is sufficient for keeping our results stable.

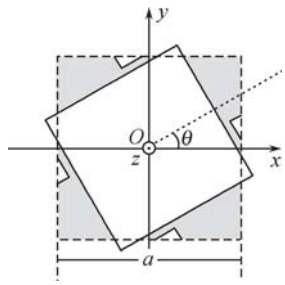

Fig. 3 Schematic view of 2-D PCs with square lattice composed of square rods in the background medium of dielectric.

Figure 4 displays the LDFs of the atoms transition frequency at the middle of the pseudo-PBG $\omega = \omega_g = 0.425(2\pi c/a)$ for emitters (a) in the air rods and (b) in background medium. The solid and dashed curves correspond, respectively, to the atomic polarization along x and z direction. In order to clearly reveal the PCs effect, the reference lifetimes in Fig. 4(a) and (b) are, respectively, taken as the values of the lifetimes of the polarized atoms in homogeneous air and background medium, which are marked by vertical dotted line at $\tilde{\tau} = 1$. It is very interesting to note that the two curves in Fig. 4(b) are almost separated by a demarcative point around $\tilde{\tau} = 2$, significantly different from Fig. 4(a). It manifests that the SE of all the emitters polarized in the x direction are inhibited intensively. The result observed in Fig. 4(b) implies a switching effect between the inhibition and enhancement of SE, which mainly originates from the polarization of the dipole moment of emitters, rather than the pseudo-PBG. In order to prove this argument, we examine the lifetime distribution for the case of the emitters transition frequency being outside the pseudo-gap. We shift the emitters transition frequency to $\omega = 0.385(2\pi c/a)$ near the band edge, but keep other parameters the same as in Fig. 4. The calculated results are displayed in Fig. 5(a). The basic profiles of the two curves are quite similar to that of the corresponding curves in Fig. 4(b), and the switching effect is observed once again. However, we also see the existence of differ-

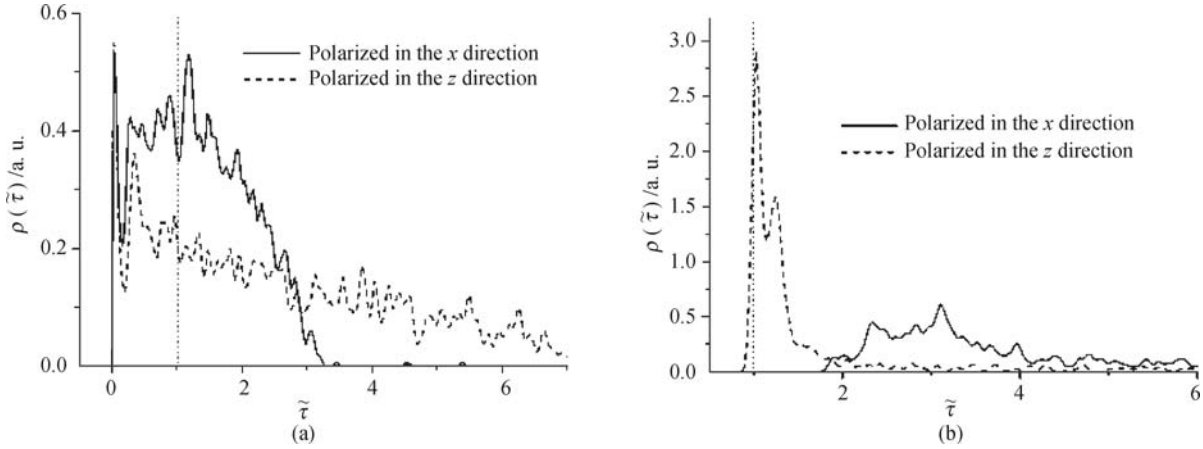

Fig. 4 LDFs of emitters polarized along the x (*solid line*) and z direction (*dashed line*) in the 2-D PCs with $\varepsilon = 12.96$, $f = 0.68$, $\theta = 30°$. The emitters are **(a)** in the air rods and **(b)** in background medium.

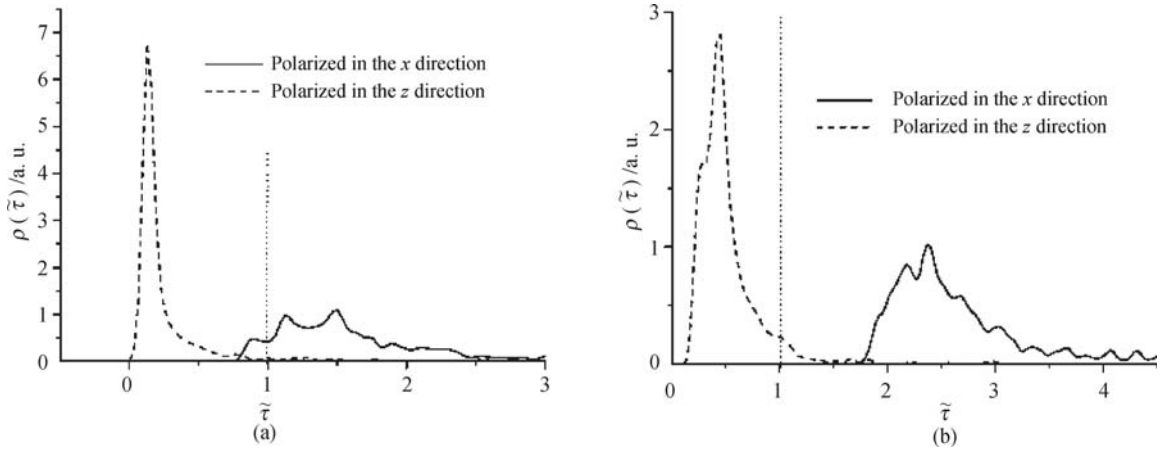

Fig. 5 LDFs of differently polarized emitters located in the dielectric medium. The parameters are the same as those in Fig. 4(b) except for **(a)** $\omega_g = 0.385(2\pi c/a)$ and **(b)** $f = 0.6$.

ences between Figs. 4(b) and 5(a): (i) the distribution curves in Fig. 5(a) are shifted towards the short lifetime region on the whole, which can be attributed to a large LDOS near the pseudo-band edge. (ii) The two curves in Fig. 5(a) are separated at a point of about $\tilde{\tau} = 0.8$. Thus, the SE of emitters polarized along the x direction is strongly suppressed, while the SE of most of the emitters polarized in the z direction is accelerated. If we change f from 0.68 to 0.6 and the other parameters are the same as those in Fig. 4(b), the emitters transition frequency $\omega = \omega_g = 0.425(2\pi c/a)$ is outside the pseudo-gap. The LDFs are displayed in Fig. 5(b). It can be seen that the two curves are completely separated. It is very favorable to the switching effect. The results in Fig. 5(a) and (b) demonstrate that the switching effect is mainly caused by the polarization of the dipole moment, rather than the pseudo-gap. This implies that we find a new degree of freedom of controlling the SE processes by tuning the polarized direction of emitters.

2.3 Lifetime distribution and decay kinetic properties in 3-D PCs

In this section, we define the lifetime distribution function as [34]:

$$\rho(\tilde{\tau}) = \sum_i W_i \delta(\tilde{\tau} - \tilde{\tau}(\boldsymbol{r}_i, \omega_0)) \tag{13}$$

$\boldsymbol{r}_i$ and W_i have the same meaning as in Eq. (12). Reference [34], based on the LDFs, studied the decay kinetics of the SE from an assembly of the emitters in PCs with pseudo-gap. The decay kinetics strongly depending on the emitters' situation and transition frequency in PCs has been shown. The concept of the single-average of SE remains generally invalid for PCs. The pure PCs' effect may cause the coexistence of both accelerated and inhibited decay processes. We provided a theoretical clarification for substantial discrepancies among the experiment results [88, 89]. We consider PCs of fcc lattice consisting of spherical globules with refractive index n in the background media with refractive index n_b [34]: $n = 2.6$, $n_b = 1.33$, and $f = 0.65$. The PCs possess pseudo-gap along the (1 1 1) direction. The lifetime distributions of the emitters in PCs are displayed in Fig. 6. Figure 6(a) shows that the observable relative width of the lifetime distribution (RWOLD) $T_{rw} = (\tau_{\max} - \tau_{\min})/\tau_{\min}$ of emitters outside dielectric spheres are high up to 600%–700%, for three different transition frequencies ω_0, correspond-

ing to lower, center, and upper edges of the pseudo-PBG, respectively. Compared with the chosen reference lifetime τ_0, the decay process for most of the emitters outside dielectric globules is remarkably accelerated. However, Fig. 6(b) reveals that the SE is substantially inhibited when emitters are embedded on the spherical surface of radius $r = 0.6r_0$ inside the dielectric spheres. We observe once again that the accelerated and inhibited decay processes of emitters simultaneously occur. The observable RWOLD T_{rw} for the emitters located on the spherical surface still remain narrower, less than 9%. Hence, the radial distribution of the lifetimes approximately characterizes the decay kinetics of the emitters in the whole dielectric spheres. Figure 6(c) displays that the RWOLD inside the dielectric spheres is large, up to 400%. The results in Fig. 6(a)–(c) demonstrate that the increase of index contrast rapidly broadens the lifetime distribution of emitters.

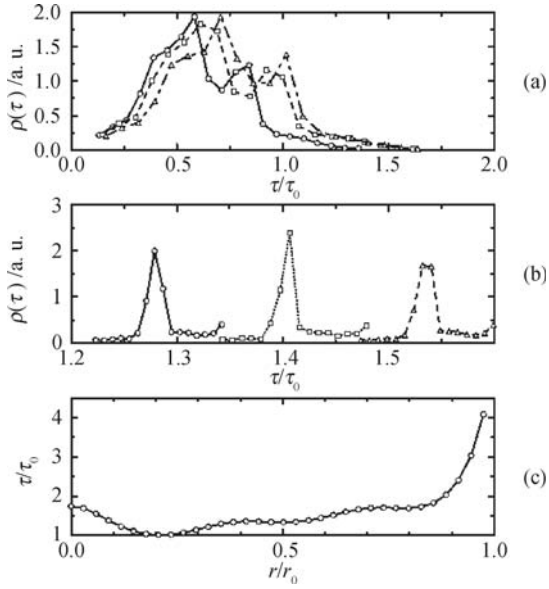

Fig. 6 Lifetime distribution of the emitters in fcc PCs: **(a)** outside the dielectric spheres and **(b)** on the spherical surface with a radius of $r = 0.6r_0$ inside the dielectric globules. In (a) and (b), the solid, dotted, and dashed lines correspond to the transition frequency $\omega_0 = 0.387(2\pi c/a)$, $\omega_0 = 0.404(2\pi c/a)$, and $\omega_0 = 0.421(2\pi c/a)$, respectively. **(c)** Variation of the lifetime with the radius of the spherical surface along the x axes direction at $\omega_0 = 0.404(2\pi c/a)$. τ_0 is the lifetime of emitters in an infinite homogeneous medium with $n = 2.6$.

We now examine the decay behavior of an excited emitter in two PC structures [35]: one is a diamond structure consisting of dielectric spheres of the refractive index $n = 3.6$ in the air background with a filling fraction $f = 0.31$, whose absolute PBGs spanning from $0.738(2\pi c/a)$ to $0.776(2\pi c/a)$ and from $0.990(2\pi c/a)$ to $1.028(2\pi c/a)$. The other is the inverse opal structure consisting of air spheres in a medium with $n = 3.6$ and $f = 0.74$, whose absolute PBG ranges from $0.756(2\pi c/a)$ to $0.780(2\pi c/a)$.

Figure 7 displays the decay behavior of an excited emitter at three different positions in the diamond structure for ω_0 located (a) outside and (b) inside the second PBG. It is evident from Fig. 7 (a) that when ω_0 is outside the PBG and near the gap edge, an excited atom at $\boldsymbol{r} = \boldsymbol{r}_1$ decays non-exponentially, while an excited atom at $\boldsymbol{r} = \boldsymbol{r}_2$ or $\boldsymbol{r} = \boldsymbol{r}_3$ decays exponentially to a good approximation. It is also clearly seen from Fig. 7(b) that when ω_0 is inside the PBG and near the gap edge, the population of the excited state of an emitter at $\boldsymbol{r} = \boldsymbol{r}_1$ or $\boldsymbol{r} = \boldsymbol{r}_2$ exhibits Rabi oscillations with a damped envelope and is rapidly trapped into a fractionalized steady-state, while this oscillatory and fractional trapping phenomenon is unobservable for an atom at $\boldsymbol{r} = \boldsymbol{r}_3$. These results show that an emitter at different positions in the PCs can have fundamentally different radiation properties.

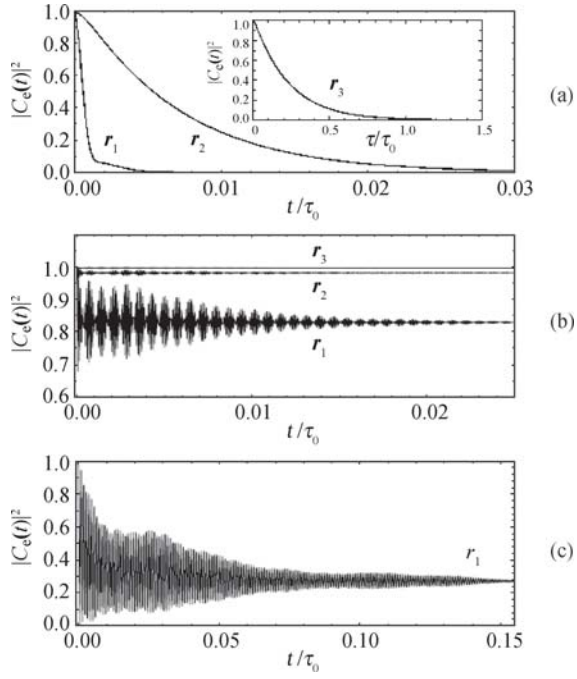

Fig. 7 Time evolution of the excited state population in the diamond structure for an emitter at three different positions, $\boldsymbol{r}_1 = (0, 0, 0)a$, $\boldsymbol{r}_2 = (0.05, -0.125, 0)a$, and $\boldsymbol{r}_3 = (0.5, 0, 0)a$. **(a)** For transition frequency $\omega_0 = 1.032(2\pi c/a)$ outside the gap and $\alpha_0 = 3 \times 10^{-5}$, **(b)** for $\omega_0 = 1.018(2\pi c/a)$ inside the gap and $\alpha_0 = 3 \times 10^{-5}$ (i.e., the case of nonresonant emission), and **(c)** for $\omega_0 = 1.018(2\pi c/a)$ and $\alpha_0 = 3 \times 10^{-4}$ (i.e., the case of resonant emission). τ_0 is the lifetime of the emitter in free space.

Figure 8 shows the time evolution of the excited-state population in the inverse-opal structure for three different emitter positions. When the transition frequency $\omega_0 = 0.745(2\pi c/a)$ is outside the PBG, an excited emitter at the three positions exhibits the well defined exponential decay behavior [Fig. 8(a)]. On the contrary, when $\omega_0 = 0.762(2\pi c/a)$ is inside the PBG, it is clearly seen that for an emitter at $\boldsymbol{r} = \boldsymbol{r}_2$ [Fig. 8(b)] the population of the excited state exhibits Rabi oscillations and approaches a steady value of 0.9675 in the long-time limit. However, for an atom at $\boldsymbol{r} = \boldsymbol{r}_1$ or $\boldsymbol{r}_3$, the oscillatory

magnitudes of the populations are extremely small, and the steady populations are 0.9985 and 0.9973, respectively.

From Fig. 7 and Fig. 8, it can be seen that the evolution spectrum inside the PBG leads to a localized field, while outside the PBG corresponds to a propagating field. The superposition of the localized field with propagating field results in Rabi oscillations and fractional trapping behavior in the population of the excited state. Obviously, the decay kinetic properties have position dependence in the PCs.

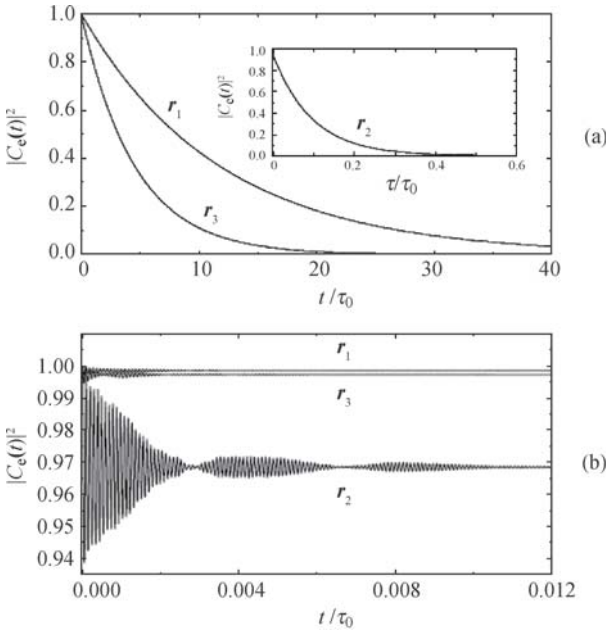

Fig. 8 Time evolution of the excited state population in the inverse-opal structure for an emitter with $\alpha_0 = 3 \times 10^{-5}$ at three different positions, $\boldsymbol{r}_1 = (0, 0, 0)a$, $\boldsymbol{r}_2 = (0.34, 0, 0)a$, and $\boldsymbol{r}_3 = (0.24, 0.24, 0)a$. **(a)** For transition frequency $\omega_0 = 0.745(2\pi c/a)$ outside the gap and **(b)** for $\omega_0 = 0.762(2\pi c/a)$ inside the gap.

The above research results on the lifetime distribution and decay kinetic properties of emitters in 2-D and 3-D PCs imply that it is possible to engineer the SE by controlling the positions and the polarized orientation of the emitters.

2.4 SE in microcavities and metallic micro- and nanostructures

Microcavities can change the optical density of states, which can affect the SE properties of the emitters. The effect was first presented by Purcell [16] (about 60 years ago) in nuclear magnetic resonance for decreasing the relaxation time. In 1981, the Purcell effect was emphasized by Kleppner [96] in the atomic case. The atom releases its energy because of its interaction with optical field, so that if the interaction could be "switched off", the atom would remain forever in its excited state. This idea in the opposite sense than Purcell is to decrease the interaction so as to increase the lifetime of excited state. Intuitively, if the dipole of the emitter is resonant with the cavity mode, the emitter sees the increased photon density of states with respect to the vacuum density of states. The SE rate is therefore enhanced: the emitter decays faster than in vacuum and the photons are emitted in the cavity mode. On the other hand, if the transition frequency of the emitter is out of resonance, namely in a photonic gap, the emitter sees the smaller photon density of states than in vacuum and the SE rate is reduced. The Purcell effect therefore perfectly illustrates the role played by an optical cavity that is to locally tailor the dipole-field coupling and the density of available photon modes. The control of SE through the Purcell effect is a good way to fabricate high performance optoelectronics and quantum information devices. In theory, this effect is quantized by Fermi's golden rule [97], which states that the SE rate depends on the density of states (DOS) of the electromagnetic field. Gérard and Kavokin briefly derive the expression of the Purcell factor [44, 47] of a 2-D and 3-D cavity through the Fermi Golden Rule, and detail its physical significance. The Purcell factor can give a quantitative interpretation of experimental results. Compared with other microcavity systems such as micropillars and microdisks, planar PCs microcavities and waveguides have the inherent advantage that they can be easily integrated on a chip to control the photons. A simple PCs cavity can be realized by adding a defect into the perfect PCs slab, for example, by removing one hole. Advanced lithography and etching techniques have recently led to major improvements in the fabrication of nanoscale planar PCs and planar PCs microcavities [98]. Hughes applied a real-space Green function tensor (GFT) technique to derive semi-quantitatively analytical expressions for enhanced emission rates in various planar PCs microcavities and waveguides structures and demonstrated that Purcell factor ($F_p > 10$) can be realized for single quantum dots (QDs) embedded in a planar-PCs waveguide [99]. Because the impact of imperfections for long waveguides will act to broaden the large SE enhanced factors and limit the proposed devices' applications, they recently designed a finite-sized waveguide structure. The rigorous Bloch analysis and analytical Green's function methods do not apply in finite-sized structure. Then they developed the numerically computing methods to compute the exact Purcell factor. Their waveguide structure and corresponding band gap are displayed in Fig. 9 [100, 101]. They also considered the other short PCs waveguide but surrounded by air only on one end and closed by a defect-free PCs on the other end (acting as a reflector) [100, 102, 103]. This structure displayed in Fig. 10 can easily realize efficient on-chip directional collection of the emitted photons. The Purcell factors versus frequency for a waveguide and waveguide-cavity is shown in Fig. 11. From Fig. 11(a), we know that the Purcell factor peak value is about 46 for a 10

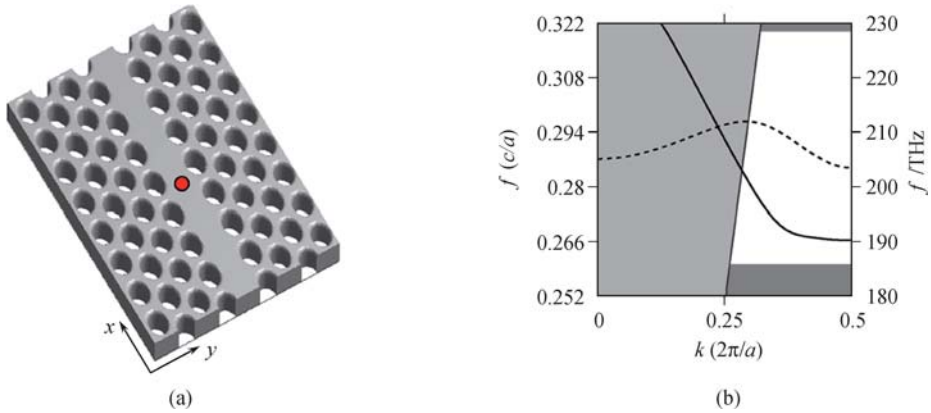

Fig. 9 **(a)** Schematic of a 10 unit-cell planar-PC waveguide (W1) along the x axis and a single quantum dot (QD: *filled red circle*) embedded at the center of the slab. **(b)** The band structure of modes (*solid and dashed curves*) corresponding to an infinite-length planar-PC waveguide shown within the TE-like band gap. The gray shaded region above the light line represents the continuum of radiation modes.

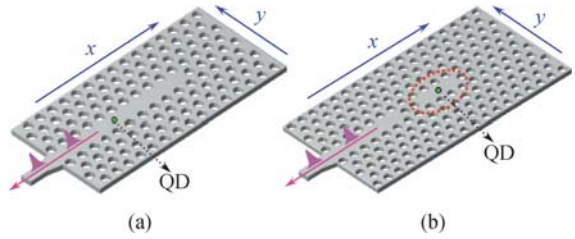

Fig. 10 Schematic diagrams of **(a)** a finite-sized PCs waveguide, **(b)** a finite-sized PCs waveguide-cavity. The green dot refers to the QD.

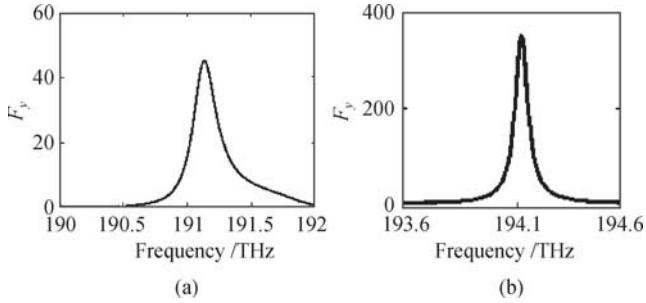

Fig. 11 Purcell factor (F_y) versus frequency for a QD embedded in **(a)** the finite-sized PCs waveguide [Fig. 10(a)] and **(b)** in a cavity, which are couple by a waveguide.

unit-cell waveguide corresponding to Fig. 10(a). For comparison, the waveguide-cavity structure [Fig. 10(b)] is also investigated, where the peaking is increased to about 350. Using this integrated waveguide-cavity systems, on chip single photon sources will be fabricated for quantum key distribution in the near future. Fussell gave another approach to demonstrate SE rate by projecting Green's tensor onto a set of quasimodes associated with the resonances. In their design structure, the SE rate peak value is 160. The SE rates following the positions are displayed in Fig. 12 [104]. Recently, Ma and John presented an atomic Bloch vector equation in a bimodal photonic band gap waveguide for ultrafast multiwavelength channel all-optical logic in PBG microchips [84]. This offers a foundation for an on-chip multichannel all-optical transistor. Unlike electronic binary logic and quantum probabilistic multivalued logic, their optical system offers the possibility of picosecond deterministic multivalued logic.

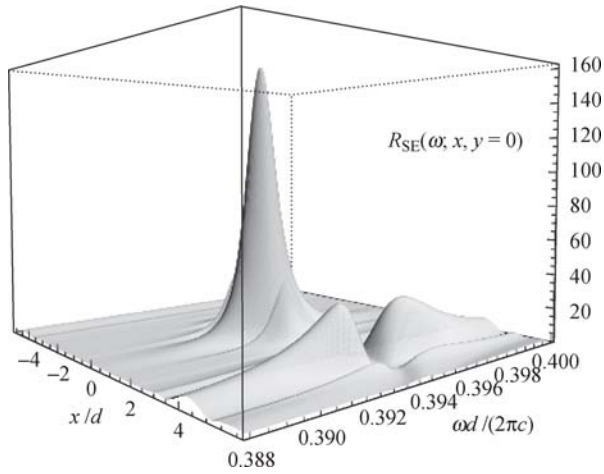

Fig. 12 SE ratio R_{SE} as a function of the frequency ω and position x along the x axis of the coupled microcavity structure.

Metallic micro- or nano-structures can provide another cavity-free approach to control the interaction between the emitter and sub-wavelength confinement of the optical field. In recent years, both experimentally and theoretically, there has been a growing interest in controlling the efficiency of SE using metallic nanostructures. To obtain more enhancements, Paiella [76] theoretically proposed to use multiple metallo-dielectric layers to engineer the surface-plasmon density of states. Purcell factor maximum value reaches up to 79 and internal quantum efficiency of LEDs can increase from 10% to 90% in multiple structures designed by them. Strong coherent coupling between guided Plasmon modes on conducting nanowires and emitters in the optical domain leads to large effective Purcell factors for emission into the Plasmon modes. This phenomenon was first illustrated by Chang [81]. Single-photon generation efficiencies exceeding 95% can be achieved in their system. However, in Refs. [78, 81], only one ($n = 0$) fundamental Plasmon mode is considered and all other modes are cutoff in the

limit of vanishing nanowire radius ($R \to 0$). Chen modified the limit and considered the interaction between other Plasmon modes with the emitter on finite radius nanowire [82, 83]. Their results are displayed in Fig. 13. Figure 13 (b) and (c) shows the rate of SE into the first few modes ($\Gamma_n, n = 0, 1, 2, 3$), which correspond to $R = 0.1$ and $R = 0.5$, respectively. In Fig. 13 (b) and (c), the distance between the emitter and the nanowire surface is fixed at $d = 10.76$ nm. From the figure we can see (i) the SE rate approach infinity at certain values of the exciton band gap; (ii) The latter modes ($n > 3$) contribute much less to the decay rate. In Koenderink's Letter, the coupling of emitters to nanosphere chains for directional single photon sources can be explained by exact electrodynamical calculations [86].

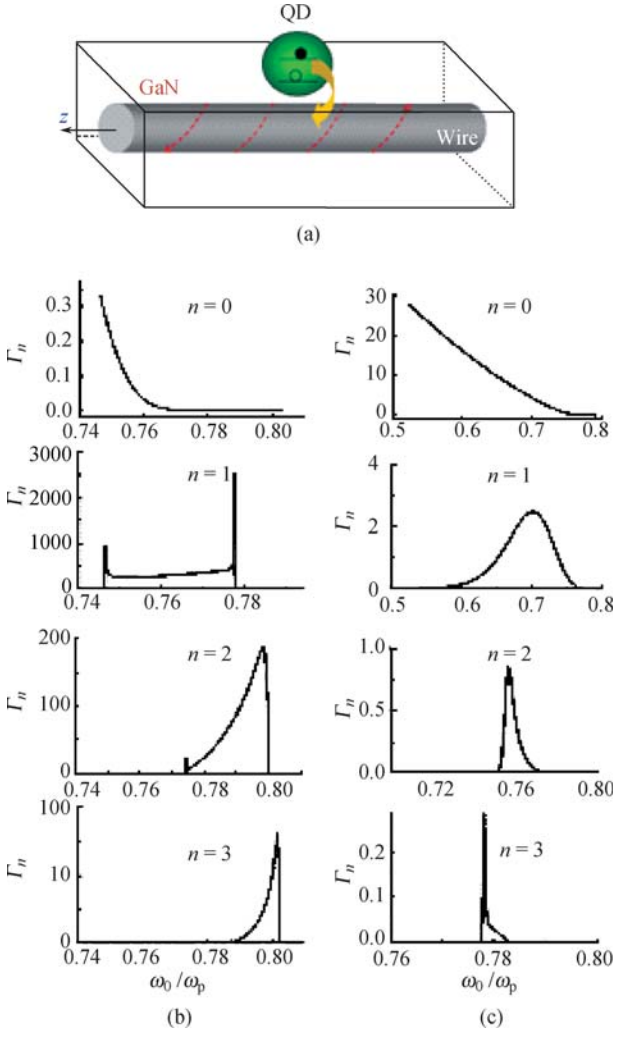

Fig. 13 **(a)** schematic view of the system. SE of a two level emitter on the nanowire. The rate (Γ_n) SE into $n = 0 - 3$ modes for **(b)** $R = 0.1$ and **(c)** $R = 0.5$. The unit of Γ_n is normalized to the free-space decay rate Γ_0.

3 Experiments on SE manipulation in micro- and nano-structures

The control of SE through the Purcell effect in the experiment is an effective way to reduce the threshold of lasers and realize single photon sources. This effect has been actively looked for with atoms placed in cavities, and with QDs placed in PCs, micropillars microcavities, microdisks microcavities or PCs microcavities. This section reviews some fundamental papers experimentally demonstrating the control over the SE properties.

3.1 SE control in photonic crystals

It is well known that the SE properties depend on the LDOS of electromagnetic fields. Because of the LDOS having strong position-dependent characteristics, PCs provide the best platform to control the SE of the emitters through tailoring the LDOS in it. To realize the SE manipulation in PCs, the major tasks include: fabrication of excellent PCs, appropriate combination of QDs with PCs and accurate positioning of the emitters. Owing to the remarkable progress achieved in nanoscience and nanotechnology, excellent PCs have been made by the state-of-the-art fabrication techniques [42, 105, 106], and QDs have been successfully combined with PCs and deterministically positioned in PCs to within 25 nm accuracy [107]. The modification of SE has been demonstrated by many groups and corresponding results can be read in the review article [42]. In this section, we are interested in the recent experimental progresses about SE control through PCs.

In 2-D PCs, Kaniber *et al.* have presented an efficient single photon generation system by controlling SE of the emitter in 2-D PCs. Compared to QD in bulk materials, the external quantum efficiency of the emitters in PCs was enhanced 16 times [108]. Lately, Chauvin [27] demonstrated the SE enhancement from emitters in the 1550 nm telecommunication window. The SE rate enhancement by a factor of 1.5–2 was observed by them.

Lodahl *et al.* [20] accomplished the first experiment to investigate the SE control in 3-D inverse opal PCs and demonstrated the decay properties of the emitters in visible light regime which depending on both the transition frequency of the emitter and the crystal's lattice parameter was shown. Their pioneering experiment results proved that 3-D PCs could provide an all-solid-state dynamics control platform for quantum information systems. Lately, Vallée [109] and Vion [25] observed strong modification of emission in opal structures with relatively low dielectric refractivity. Although the experimental progress made in SE control with opals and inverse opals PCs is encouraging, the work wavelength in visible light regime is a limitation for future application in telecommunications.

Li *et al.* [22], for the first time, observed significant modifications in both the emission spectra and SE lifetime of emitters infiltrated in the 3-D woodpile PCs fabricated by two-photon polymerization methods. In

their experiment, they observed the weak inhibition of SE by up to ∼ 20%. Their work makes an important progress for manipulating SE in the near-infrared wavelength regime through 3-D PCs, which can provide a state-of-the-art platform for active devices in telecommunication. Ventura *et al.* [24] fabricated 3-D woodpile PCs using PbSe QD-doped nanocomposite polymer material. The SE inhibition in the band gap and enhancement near the band edges were presented (see Fig. 14). Their experiment can be explained by the reduction of modes in a band gap and an increase of modes near the band edges. Recently, Hippo [110] using Time-Resolve photoluminescence measurements technique found that the excited states lifetime of silicon nanocrystals on 3-D silicon PCs decrease at 750 nm and increase at 800 nm compared to those on the silicon substrate without 3-D PCs. Their experiment results reveal that the SE control of silicon nanocrystals has been realized using 3-D PCs.

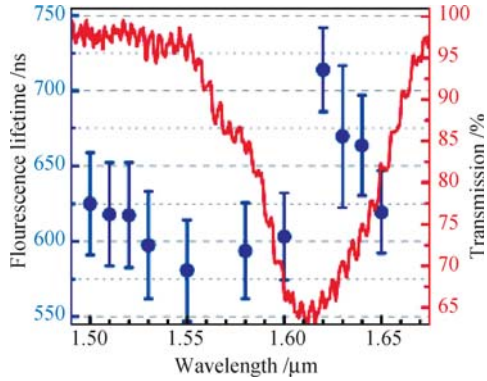

Fig. 14 Fluorescence lifetime of the emitters doped in a 3-D woodpile PCs with a band gap at the wavelength 1.61 μm. Blue dot and red curve correspond to lifetime and band gap, respectively. The lifetime at wavelength 1510 μm away from the band gap is 625 ns. As the wavelength approaches the band gap, the lifetime is reduced to 590 ns at wavelength 1580 nm. This proves the SE enhancement near the band gap. Towards the center of the band gap at wavelength 1611 nm, an evident increase of lifetime is observed. This proves the SE inhabitation in the band gap.

By 2-D slab PCs, Fujita *et al.* [39] demonstrated the strong controlling SE of quantum well. At the frequencies in the band gap of the slab PCs, a fivefold increased decay lifetime is measured in the in-plane direction. For the same frequencies enhanced emission effect is observed in the vertical modes. These phenomena reveal the redistribution of SE. Lately, Kounoike *et al.* [111] also found that the SE lifetime of QDs in a 2-D slab PCs increase up to 15-fold and emission efficiency in the vertical direction was simultaneously increased 15-fold by redistribution. Their experiments show that using 2-D slab PCs can manipulate the SE of QDs.

3.2 SE control in microcavities and metallic nanostructures

For an optical microcavity, Goy *et al.* [112] reported the first experimental result of Purcell enhancement of atoms. Four years later, Martini [113] demonstrated the result of lifetime enhancement 300%. Recently, Steiner, for the first time, showed cavity-controlled decay curves and fluorescence spectra of the single dye molecule placed in a fixed position inside a $\lambda/2$ microcavity and revealed that the Purcell factor increased up to 2.7 [114].

Embedding QDs in a pillar cavity, Gérard and Gayral [47] first reported the shortening or lengthening of the lifetime in the SE problem and demonstrated a Purcell factor of 5. The Purcell enhancement of SE, a much quicker decay in resonance and delay decay in out of resonance are displayed in Fig. 15 [46]. Another experiment given by Bayer [49], in a pillar whose sides had been coated or not, demonstrated the impact of leaky emission on the Purcell effect. Solomon [48] found that a single QD SE lifetime is reduced from the noncavity value of 1.3 ns to 280 ps. Schwab [115] presented that the altered SE depends on excitation intensity. Adawi [116] and Bennett [117] also found Purcell effect in pillar microcavity. Recently, using a QD weakly coupled to a micropillar cavity, a single photon sources with an indistinguishability of 90% was reported by Ates [118].

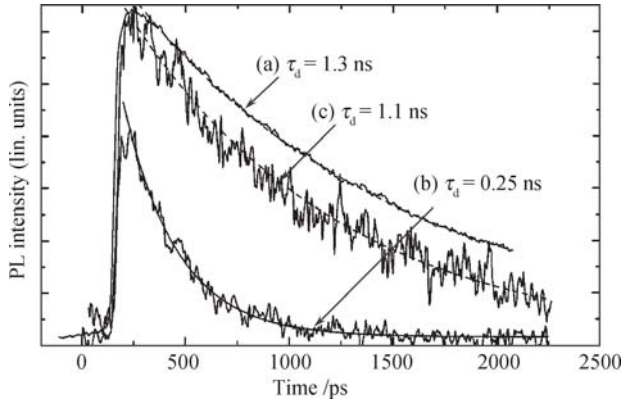

Fig. 15 Time-resolved photoluminescence of a quantum emitter embedded **(a)** in bulk GaAs matrix, and **(b)** in resonance and **(c)** out of resonance in a pillar microcavity. In case (b) the decay is about five times quicker than in case (a). (c) displays only a small enhancement of SE lifetime compared to (a).

For quantum emitters embedded in microdisks, a shortening of the excitation state decay by a factor of up to 12 was observed by Gayral [51]. For both on-resonance and off-resonance QDs, the decay curves are shown in Fig. 16. For off-resonance QDs, the PL decay curve is monoexponential, the decay time being 1.2 ns. The decay lifetime is much faster for on-resonance QDs. The decay time 105 ps and 12 times faster than the vacuum decay were given for the QD in microcavity with Q = 10 000. Kiraz [52] demonstrated exciton lifetime reduction by 6 due to the Purcell effect by tuning the QD into resonance with the microdisks cavity. Fang [53] studied the enhancement of SE rate for InAs QDs embedded in GaAs microdisks in a time-resolved photoluminescence experiment and reported an SE en-

hancement factor exceeding 10.

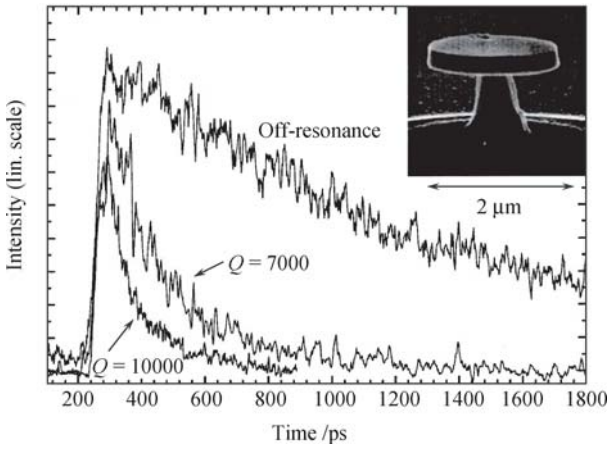

Fig. 16 Time-resolved photoluminescence signal of QDs in a microdisk. The decay for spectrally off-resonance QD is monoexponential with a decay time of 1.2 ns. If we now consider on-resonance QD with the cavity mode, here for two different microdisks with $Q = 7000$ and $Q = 10\ 000$, the decay is clearly much faster. The inset shows a scanning electron microscopy picture of a microdisk.

PCs nanocavities offer a scalable platform for quantum optics experiments and the potential applications in quantum information processing, so QDs in PC nanocavities system have progressed rapidly. Happ [119] and Kress [120] observed a Purcell enhancement with the shortening of emission lifetime 9 and 19 in 2-D PCs nanocavities, respectively. Englund [54], Chang [10] and Kaniber [121, 122] demonstrated the single photon sources and Strauf [123] showed the PCs laser based high-quality QDs and nanocavities systems. Balet [124] illustrated coupling at optical communication regime 1.3 μm between single InAs QDs and a mode of a two-dimensional PCs defect cavity. They performed a time integrated and time-resolved photoluminescence and measured an eightfold increase in the SE rate inducing a coupling efficiency of 96%. In Fig. 17, Purcell effect is nicely demonstrated by Balet [124] who observed that the SE lifetime of a QD away from cavity (corresponding dot in a bulk semiconductor) is 1.2 ns. When a similar dot is detuned 2.5 μm from the cavity, its lifetime is extended to 3.6 ns, while still another dot — in resonance with a cavity mode — sees its lifetime drop to 150 ps.

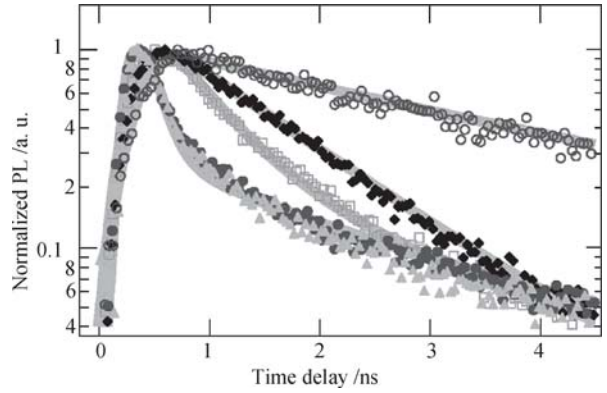

Fig. 17 Time resolved dynamics of QD off resonance (*empty red circles*), of QD in bulk (*empty blue squares*) and of QD on resonance with the cavity mode (*filled red circles*).

Lately, Francardi *et al.* [125] observed the enhancement SE of a PCs LEDs at the same wavelength as Balet. Fujita demonstrated that employing a PCs nanocavity in silicon can greatly improve the light extraction efficiency, the characteristics of the radiation pattern, and the internal quantum efficiency [126]. Recently, Gong [127] studied the light emission at 1.54 μm from an Er-doped amorphous silicon nitride layer coupled to PCs nanocavities at cryogenic and room temperatures. Their measurements gave from 11- to 17-fold Purcell enhancements of SE at cryogenic temperatures, and 2.4 fold enhancement at room temperature. The SE enhancement effect was also observed in PCs wire [128] and a PCs double-heterostructure nanocavity [55].

The light emission properties of quantum well stacking in 3-D woodpile PCs have been investigated by Ogawa [19]. The strong emission properties of the emitter in PCs with a point defect were found compared with the emission from the PCs without a defect. The results show that a single emission peak can be observed for the smallest defect and the shape of a defect also affected the emission characteristics. By comparing the SE properties with those in Ref. [19], Ogawa fabricated a 17 stacked layers woodpile 3-D PCs structure containing a quantum well emitter and a defect cavity [23]. The maximum SE emission intensity attenuation was –30 dB. In Ref. [19], the maximum suppression was limited to –20 dB.

In recent years, there has been a growing interest in the interaction of emitters with metallic nanostructures. The emission properties can be dramatically modified by the metallic nanostructures. Neogi *et al.* [72, 74] have demonstrated the decay of SE from quantum well and QDs near a silver thin film. Chen [129] also found the Purcell enhancements of quantum well near a Ag film. Akimov [80] and Fedudik [130] demonstrated efficient exciton-plasmon-photon conversion using QDs placed near the silver nanowire. These remarkable achievements have many exciting prospects, such as the realization of single photon transistors [79]. Recently, Oulton *et al.* [131] demonstrated the nanometer-scale plasmonic lasers using a hybrid plasmonic waveguide consisting of a high cadmium sulphide semiconductor nanowire separated from a silver surface.

4 Conclusions and outlook

In this review, the position-dependent photon-emitter interaction theory based upon the Green's function method of the evolution operator is briefly introduced to analyze the SE behaviors of emitters in defect-free 2-D and 3-D PCs. It is demonstrated that the concept of the

single-averaged-lifetime of SE remains generally invalid for PCs, and the PCs effect may cause the coexistence of both the accelerated and inhibited decay processes. Then, we have surveyed the theoretical and experimental advance in the SE control in micro- and nano-structures such as PC waveguides, nano cavities, and metal nano structures. Some important applications of the SE control, such as nano-lasers, single photon sources, high performance LEDs, and quantum information processing devices, have also been reviewed. It is worthy to point out that there are still great challenges in the SE control, in fabricating high quality micro- or nano-structures and deterministically positioning a single QD inside micro- or nano-structures. However, we believe, with the development of technology, that the challenges will be overcome in the near future.

Acknowledgements The authors acknowledged the financial support from the Chinese National Key Basic Research Special Fund (Grant Nos. 2006CB921706 and 2010CB923200) and the National Natural Science Foundation of China (Grant Nos. 10725420 and U0934002).

References

1. A. Mihi, F. J. Lopez-Alcaraz, and H. Miguez, Appl. Phys. Lett., 2006, 88(19): 193110
2. A. Mihi, S. Colodrero, M. Calvo, M. Ocana, and H. Miguez, Enhanced Power Conversion Efficiency in Solar Cells Coupled to Photonic Crystals, edited by M. W. Sharon, S. S. Ganapathi, and G. S. Florencio, SPIE, 2007: 664007
3. Y. Park, E. Drouard, O. El Daif, X. Letartre, P. Viktorovitch, A. Fave, A. Kaminski, M. Lemiti, and C. Seassal, Opt. Express, 2009, 17(16): 14312
4. D. H. Ko, J. R. Tumbleston, L. Zhang, S. Williams, J. M. DeSimone, R. Lopez, and E. T. Samulski, Nano Lett., 2009, 9(7): 2742
5. S. Colodrero, A. Mihi, J. A. Anta, M. Ocaña, and H. Míguez, J. Phys. Chem. C, 2009, 113(4): 1150
6. C. Santori, M. Pelton, G. Solomon, Y. Dale, and Y. Yamamoto, Phys. Rev. Lett., 2001, 86: 1502
7. C. Santori, D. Fattal, J. Vucković, G. S. Solomon, and Y. Yamamoto, Nature, 2002, 419(6907): 594
8. P. Michler, A. Kiraz, C. Becher, W. V. Schoenfeld, P. M. Petroff, L. Zhang, E. Hu, and A. Imamoglu, Science, 2000, 290(5500): 2282
9. M. Keller, B. Lange, K. Hayasaka, W. Lange, and H. Walther, Nature, 2004, 431(7012): 1075
10. W. H. Chang, W. Y. Chen, H. S. Chang, T. P. Hsieh, J. I. Chyi, and T. M. Hsu, Phys. Rev. Lett., 2006, 96: 117401
11. S. Strauf, N. G. Stoltz, M. T. Rakher, L. A. Coldren, P. M. Petroff, and D. Bouwmeester, Nature Photonics, 2007, 1(12): 704
12. M. Toishi, D. Englund, A. Faraon, and J. Vucković, Opt. Express, 2009, 17(17): 14618
13. J. Claudon, J. Bleuse, N. S. Malik, M. Bazin, P. Jaffrennou, N. Gregersen, C. Sauvan, P. Lalanne, and J. M. Gérard, Nature Photonics, 2010, 4(3): 174
14. J. J. Wierer, A. David, and M. M. Megens, Nature Photonics, 2009, 3(3): 163
15. H. G. Park, S. H. Kim, S. H. Kwon, Y. G. Ju, J. K. Yang, J. H. Baek, S. B. Kim, and Y. H. Lee, Science, 2004, 305(5689): 1444
16. E. M. Purcell, H. Torrey, and R. Pound, Phys. Rev., 1946, 69: 681
17. E. Yablonovitch, Phys. Rev. Lett., 1987, 58: 2059
18. S. John, Phys. Rev. Lett., 1987, 58: 2486
19. S. Ogawa, M. Imada, S. Yoshimoto, M. Okano, and S. Noda, Science, 2004, 305(5681): 227
20. P. Lodahl, A. Floris Van Driel, I. S. Nikolaev, A. Irman, K. Overgaag, D. Vanmaekelbergh, and W. L. Vos, Nature, 2004, 430(7000): 654
21. R. A. L. Vallee, K. Baert, B. Kolaric, M. Van der Auweraer, and K. Clays, Phys. Rev. B, 2007, 76(4): 045113
22. J. Li, B. Jia, G. Zhou, C. Bullen, J. Serbin, and M. Gu, Adv. Mater., 2007, 19(20): 3276
23. S. Ogawa, K. Ishizaki, T. Furukawa, and S. Noda, Electron. Lett., 2008, 44(5): 377
24. M. J. Ventura and M. Gu, Adv. Mater., 2008, 20(7): 1329
25. C. Vion, C. Barthou, P. Bénalloul, C. Schwob, L. Coolen, A. Gruzintev, G. Emel'chenko, V. Masalov, J. M. Frigerio, and A. Maître, J. Appl. Phys., 2009, 105(11): 113120
26. A. Ródenas, G. Zhou, D. Jaque, and M. Gu, Adv. Mater., 2009, 21(34): 3526
27. N. Chauvin, P. Nedel, C. Seassal, B. Ben Bakir, X. Letartre, M. Gendry, A. Fiore, and P. Viktorovitch, Phys. Rev. B, 2009, 80: 045315
28. S. John and T. Quang, Phys. Rev. A, 1994, 50: 1764
29. A. G. Kofman, G. Kurizki, and B. Sherman, J. Mod. Opt., 1994, 41(2): 353
30. S. Y. Zhu, H. Chen, and H. Huang, Phys. Rev. Lett., 1997, 79: 205
31. S. Y. Zhu, Y. Yang, H. Chen, H. Zheng, and M. S. Zubairy, Phys. Rev. Lett., 2000, 84: 2136
32. Z. Y. Li, L. L. Lin, and Z. Q. Zhang, Phys. Rev. Lett., 2000, 84: 4341
33. D. G. Angelakis, P. L. Knight, and E. Paspalakis, Contemp. Phys., 2004, 45(4): 303
34. X. H. Wang, R. Wang, B. Y. Gu, and G. Z. Yang, Phys. Rev. Lett., 2002, 88: 093902
35. X. H. Wang, B. Y. Gu, R. Wang, and H. Q. Xu, Phys. Rev. Lett., 2003, 91: 113904
36. Y. S. Zhou, X. H. Wang, B. Y. Gu, and F. H. Wang, Phys. Rev. E, 2005, 72: 017601
37. Y. S. Zhou, X. H. Wang, B. Y. Gu, and F. H. Wang, Phys. Rev. Lett., 2006, 96: 103601
38. S. C. Cheng, J. N. Wu, M. R. Tsai, and W. F. Hsieh, J. Phys.: Condens. Matter, 2009, 21(1): 015503
39. M. Fujita, S. Takahashi, Y. Tanaka, T. Asano, and S. Noda, Science, 2005, 308(5726): 1296
40. M. Fujita, S. Takahashi, T. Asano, Y. Tanaka, K. Kounoike, M. Yamaguchi, J. Nakanishi, W. Stumpf, and S. Noda, J.

Opt. A, 2006, 8(4): S131
41. M. Fujita, et al., Controlling Spontaneous Emission Phenomena in Defect-free 2-D Photonic Crystals with Quantum Dots, Conference on Lasers and Electro-Optics and 2006 Quantum Electronics and Laser Science Conference, CLEO/QELS, 2006
42. S. Noda, M. Fujita, and T. Asano, Nature Photonics, 2007, 1(8): 449
43. K. J. Vahala, Nature, 2003, 424(6950): 839
44. A. V. Kavokin, J. J. Baumberg, G. Malpuech, and F. P. Laussy, Microcavities, New York: Oxford University Press Inc., 2007, Chapter 1: 1
45. P. R. Berman, Cavity Quantum Electrodynamics, San Diego: Academic Press Inc., 1994: 203–266
46. J. M. Gérard, B. Sermage, B. Gayral, B. Legrand, E. Costard, and V. Thierry-Mieg, Phys. Rev. Lett., 1998, 81: 1110
47. J. M. Gérard and B. Gayral, J. Lightwave Technol., 1999, 17(11): 2089
48. G. S. Solomon, M. Pelton, and Y. Yamamoto, Phys. Rev. Lett., 2001, 86: 3903
49. M. Bayer, T. L. Reinecke, F. Weidner, A. Larionov, A. McDonald, and A. Forchel, Phys. Rev. Lett., 2001, 86: 3168
50. M. Munsch, A. Mosset, A. Auffèves, S. Seidelin, J. Poizat, J. M. Gérard, A. Lemaître, I. Sagnes, and P. Senellart, Phys. Rev. B, 2009, 80: 115312
51. B. Gayral, J. M. Gérard, B. Sermage, A. Lemaitre, and C. Dupuis, Appl. Phys. Lett., 2001, 78(19): 2828
52. A. Kiraz, P. Michler, C. Becher, B. Gayral, A. Imamoğlu, L. Zhang, E. Hu, W. V. Schoenfeld, and P. M. Petroff, Appl. Phys. Lett., 2001, 78(25): 3932
53. W. Fang, J. Y. Xu, A. Yamilov, H. Cao, Y. Ma, S. T. Ho, and G. S. Solomon, Opt. Lett., 2002, 27(11): 948
54. D. Englund, D. Fattal, E. Waks, G. Solomon, B. Zhang, T. Nakaoka, Y. Arakawa, Y. Yamamoto, and J. Vucković, Phys. Rev. Lett., 2005, 95: 013904
55. W. C. Stumpf, M. Fujita, M. Yamaguchi, T. Asano, and S. Noda, Appl. Phys. Lett., 2007, 90(23): 231101
56. D. G. Gevaux, et al., Controlling spontaneous emission from quantum dots using photonic crystal microcavities, Physica Status Solidi C – Current Topics in Solid State Physics, Vol 3, No 11, edited by M. Stutzmann, Weinheim: Wiley-VCH, 2006, Vol. 3: 3676–3679
57. H. Mabuchi and A. C. Doherty, Science, 2002, 298(5597): 1372
58. A. Boca, R. Miller, K. M. Birnbaum, A. D. Boozer, J. McKeever, and H. J. Kimble, Phys. Rev. Lett., 2004, 93: 233603
59. J. P. Reithmaier, G. Sek, A. Löffler, C. Hofmann, S. Kuhn, S. Reitzenstein, L. V. Keldysh, V. D. Kulakovskii, T. L. Reinecke, and A. Forchel, Nature, 2004, 432(7014): 197
60. S. Münch, S. Reitzenstein, P. Franeck, A. Löffler, T. Heindel, S. Höfling, L. Worschech, and A. Forchel, Opt. Express, 2009, 17(15): 12821
61. C. Kistner, T. Heindel, C. Schneider, A. Rahimi-Iman, S. Reitzenstein, S. Höfling, and A. Forchel, Opt. Express, 2008, 16(19): 15006
62. S. Reitzenstein, S. Münch, P. Franeck, A. Rahimi-Iman, A. Löffler, S. Höfling, L. Worschech, and A. Forchel, Phys. Rev. Lett., 2009, 103: 127401
63. E. Peter, P. Senellart, D. Martrou, A. Lemaître, J. Hours, J. M. Gérard, and J. Bloch, Phys. Rev. Lett., 2005, 95: 067401
64. B. Dayan, A. S. Parkins, T. Aoki, E. P. Ostby, K. J. Vahala, and H. J. Kimble, Science, 2008, 319(5866): 1062
65. K. Srinivasan and O. Painter, Nature, 2007, 450(7171): 862
66. D. Englund, A. Faraon, I. Fushman, N. Stoltz, P. Petroff, and J. Vucković, Nature, 2007, 450(7171): 857
67. T. Yoshie, A. Scherer, J. Hendrickson, G. Khitrova, H. M. Gibbs, G. Rupper, C. Ell, O. B. Shchekin, and D. G. Deppe, Nature, 2004, 432(7014): 200
68. A. Faraon, I. Fushman, D. Englund, N. Stoltz, P. Petroff, and J. Vučković, Nature Physics, 2008, 4(11): 859
69. I. Fushman, D. Englund, A. Faraon, N. Stoltz, P. Petroff, and J. Vuckovic, Science, 2008, 320(5877): 769
70. G. Khitrova, H. M. Gibbs, M. Kira, S. W. Koch, and A. Scherer, Nature Physics, 2006, 2(2): 81
71. J. P. Reithmaier, Semicond. Sci. Technol., 2008, 23(12): 123001
72. A. Neogi, C. W. Lee, H. Everitt, T. Kuroda, A. Tackeuchi, and E. Yablonovitch, Phys. Rev. B, 2002, 66: 153305
73. J. Feng, T. Okamoto, and S. Kawata, Opt. Lett., 2005, 30(17): 2302
74. A. Neogi, H. Morkoç, T. Kuroda, and A. Tackeuchi, Opt. Lett., 2005, 30(1): 93
75. K. Y. Yang, K. C. Choi, and C. W. Ahn, Appl. Phys. Lett., 2009, 94(17): 173301
76. R. Paiella, Appl. Phys. Lett., 2005, 87(11): 111104
77. G. Sun, J. B. Khurgin, and R. A. Soref, Appl. Phys. Lett., 2007, 90(11): 111107
78. D. E. Chang, A. S. Sørensen, P. R. Hemmer, and M. D. Lukin, Phys. Rev. Lett., 2006, 97: 053002
79. D. E. Chang, A. S. Sørensen, E. A. Demler, and M. D. Lukin, Nature Physics, 2007, 3(11): 807
80. A. V. Akimov, A. Mukherjee, C. L. Yu, D. E. Chang, A. S. Zibrov, P. R. Hemmer, H. Park, and M. D. Lukin, Nature, 2007, 450(7168): 402
81. D. E. Chang, A. S. Sørensen, P. R. Hemmer, and M. D. Lukin, Phys. Rev. B, 2007, 76: 035420
82. G. Y. Chen, Y. N. Chen, and D. S. Chuu, Opt. Lett., 2008, 33(19): 2212
83. Y. N. Chen, G. Y. Chen, D. S. Chuu, and T. Brandes, Phys. Rev. A, 2009, 79: 033815
84. I. D. Rukhlenko, D. Handapangoda, M. Premaratne, A. V. Fedorov, A. V. Baranov, and C. Jagadish, Opt. Express, 2009, 17(20): 17570
85. A. Trügler and U. Hohenester, Phys. Rev. B, 2008, 77: 115403
86. A. F. Koenderink, Nano Lett., 2009, 9(12): 4228
87. X. H. Wang, B. Y. Gu, and Y. S. Kivshar, Sci. Technol. Adv. Mater., 2005, 6(7): 814
88. E. P. Petrov, V. N. Bogomolov, I. I. Kalosha, and S. V.

Gaponenko, Phys. Rev. Lett., 1998, 81: 77
89. M. Megens, J. E. G. J. Wijnhoven, A. Lagendijk, and W. L. Vos, Phys. Rev. A, 1999, 59: 4727
90. M. Megens, H. P. Schriemer, A. Lagendijk, and W. L. Vos, Phys. Rev. Lett., 1999, 83: 5401
91. E. P. Petrov, V. N. Bogomolov, I. I. Kalosha, and S. V. Gaponenko, Phys. Rev. Lett., 1999, 83: 5402
92. K. M. Ho, C. T. Chan, and C. M. Soukoulis, Phys. Rev. Lett., 1990, 65: 3152
93. C. Cohen-Tannoudji, J. Dupont-Roc, and G. Grynberg, Atom–Photon Interaction: Basic Processes and Applications, 1992, Chapter 3: 165–256
94. R. Wang, X. H. Wang, B. Y. Gu, and G. Z. Yang, Phys. Rev. B, 2003, 67: 155114
95. R. Wang, X. H. Wang, B. Y. Gu, and G. Z. Yang, J. Appl. Phys., 2001, 90(9): 4307
96. D. Kleppner, Phys. Rev. Lett., 1981, 47: 233
97. E. Fermi, Rev. Mod. Phys., 1932, 4: 87
98. Y. Akahane, T. Asano, B. S. Song, and S. Noda, Nature, 2003, 425(6961): 944
99. S. Hughes, Opt. Lett., 2004, 29(22): 2659
100. V. S. Rao and S. Hughes, Phys. Rev. Lett., 2007, 99: 193901
101. V. S. Rao and S. Hughes, Opt. Lett., 2008, 33(14): 1587
102. P. Yao, V. S. C. M. Rao, and S. Hughes, Laser and Photonics Reviews, DOI: 10.1002/lpor.200810081, 2009: 1–18
103. P. Yao and S. Hughes, Phys. Rev. B, 2009, 80: 165128
104. D. P. Fussell, M. M. Dignam, M. J. Steel, C. M. de Sterke, and R. C. McPhedran, Phys. Rev. A, 2006, 74: 043806
105. M. Gu, B. Jia, J. Li, and Ventura M. J., Laser & Photonics Reviews, 2009
106. S. Takahashi, K. Suzuki, M. Okano, M. Imada, T. Nakamori, Y. Ota, K. Ishizaki, and S. Noda, Nature Materies, 2009, 8: 721
107. A. Badolato, K. Hennessy, M. Atatüre, J. Dreiser, E. Hu, P. M. Petroff, and A. Imamoglu, Science, 2005, 308(5725): 1158
108. M. Kaniber, A. Laucht, T. Hürlimann, M. Bichler, R. Meyer, M. C. Amann, and J. Finley, Phys. Rev. B, 2008, 77: 073312
109. R. A. L. Vallée, K. Baert, B. Kolaric, M. Van der Auweraer, and K. Clays, Phys. Rev. B, 2007, 76: 045113
110. D. Hippo, K. Urakawa, Y. Tsuchiya, H. Mizuta, N. Koshida, and S. Oda, Mater. Chem. Phys., 2009, 116(1): 107
111. K. Kounoike, M. Yamaguchi, M. Fujita, T. Asano, J. Nakanishi, and S. Noda, Electron. Lett., 2005, 41(25): 1402
112. P. Goy, J. M. Raimond, M. Gross, and S. Haroche, Phys. Rev. Lett., 1983, 50: 1903
113. G. Innocenti, G. R. Jacobovitz, P. Mataloni, and P. Mataloni, Phys. Rev. Lett., 1987, 59: 2955
114. M. Steiner, F. Schleifenbaum, C. Stupperich, A. Virgilio Failla, A. Hartschuh, and A. J. Meixner, ChemPhysChem, 2005, 6(10): 2190
115. M. Schwab, H. Kurtze, T. Auer, T. Berstermann, M. Bayer, J. Wiersig, N. Baer, C. Gies, F. Jahnke, J. Reithmaier, A. Forchel, M. Benyoucef, and P. Michler, Phys. Rev. B, 2006, 74: 045323
116. A. M. Adawi, A. Cadby, L. G. Connolly, W.C. Hung, R. Dean, A. Tahraoui, A. M. Fox, A. G. Cullis, D. Sanvitto, M. S. Skolnick, and D. G. Lidzey, Adv. Mater., 2006, 18(6): 742
117. A. J. Bennett, D. J. P. Ellis, A. J. Shields, P. Atkinson, I. Farrer, and D. A. Ritchie, Appl. Phys. Lett., 2007, 90: 191911
118. S. Ates, S. M. Ulrich, S. Reitzenstein, A. Löffler, A. Forchel, and P. Michler, Phys. Rev. Lett., 2009, 103: 167402
119. T. D. Happ, I. Tartakovskii, V. Kulakovskii, J.P. Reithmaier, M. Kamp, and A. Forchel, Phys. Rev. B, 2002, 66: 041303
120. A. Kress, F. Hofbauer, N. Reinelt, M. Kaniber, H. Krenner, R. Meyer, G. Böhm, and J. Finley, Phys. Rev. B, 2005, 71: 241304
121. M. Kaniber, A. Kress, A. Laucht, M. Bichler, R. Meyer, M. C. Amann, and J. J. Finley, Appl. Phys. Lett., 2007, 91(6): 061106
122. M. Kaniber, A. Laucht, A. Neumann, J. Villas-Bôas, M. Bichler, M. C. Amann, and J. Finley, Phys. Rev. B, 2008, 77: 161303
123. S. Strauf, K. Hennessy, M. T. Rakher, Y. S. Choi, A. Badolato, L. C. Andreani, E. L. Hu, P. M. Petroff, and D. Bouwmeester, Phys. Rev. Lett., 2006, 96: 127404
124. L. Balet, M. Francardi, A. Gerardino, N. Chauvin, B. Alloing, C. Zinoni, C. Monat, L. H. Li, N. Le Thomas, R. Houdré, and A. Fiore, Appl. Phys. Lett., 2007, 91(12): 123115
125. M. Francardi, L. Balet, A. Gerardino, N. Chauvin, D. Bitauld, L. H. Li, B. Alloing, and A. Fiore, Appl. Phys. Lett., 2008, 93(14): 143102
126. M. Fujita, Y. Tanaka, and S. Noda, IEEE J. Sel. Top. Quantum Electron., 2008, 14(4): 1090
127. Y. Gong, M. Makarova, S. Yerci, R. Li, M. J. Stevens, B. Baek, S. W. Nam, R. H. Hadfield, S. N. Dorenbos, V. Zwiller, J. Vuckovic, and L. D. Negro, Opt. Express, 2010, 18(3): 2601
128. E. Viasnoff-Schwoob, C. Weisbuch, H. Benisty, S. Olivier, S. Varoutsis, I. Robert-Philip, R. Houdré, and C. J. Smith, Phys. Rev. Lett., 2005, 95: 183901
129. C. Y. Chen, Y. C. Lu, D. M. Yeh, and C. C. Yang, Appl. Phys. Lett., 2007, 90(18): 183114
130. Y. Fedutik, V. V. Temnov, O. Schöps, U. Woggon, and M. V. Artemyev, Phys. Rev. Lett., 2007, 99: 136802
131. R. F. Oulton, V. J. Sorger, T. Zentgraf, R. M. Ma, C. Gladden, L. Dai, G. Bartal, and X. Zhang, Nature, 2009, 461(7264): 629